Single-particle spatial dispersion and clusters in nuclei

Ebran, J.-P.; Khan, E.; Lasseri, R.-D.; Vretenar, D.

Rapid Communications

Single-particle spatial dispersion and clusters in nuclei

J.-P. Ebran,[1] E. Khan,[2] R.-D. Lasseri,[2] and D. Vretenar[3]
[1]*CEA, DAM, DIF, F-91297 Arpajon, France*
[2]*Institut de Physique Nucléaire, Université Paris-Sud, IN2P3-CNRS, Université Paris-Saclay, F-91406 Orsay Cedex, France*
[3]*Department of Physics, Faculty of Science, University of Zagreb, 10000 Zagreb, Croatia*

(Received 23 March 2018; revised manuscript received 17 April 2018; published 14 June 2018)

The spatial dispersion of the single-nucleon wave functions is analyzed using the self-consistent mean-field framework based on nuclear energy density functionals and with the harmonic-oscillator approximation for the nuclear potential. It is shown that the dispersion depends on the radial quantum number n but displays only a very weak dependence on the orbital angular momentum. An analytic expression is derived for the localization parameter that explicitly takes into account the radial quantum number of occupied single-nucleon states. The conditions for single-nucleon localization and formation of cluster structures are fulfilled in relatively light nuclei with $A \leqslant 30$ and $n = 1$ states occupied. Heavier nuclei exhibit the quantum liquid phase of nucleonic matter because occupied levels that originate from $n > 1$ spherical states are largely delocalized. Nevertheless, individual α-like clusters can be formed from valence nucleons filling single-particle levels originating from $n = 1$ spherical mean-field states.

DOI: 10.1103/PhysRevC.97.061301

Nucleon localization and formation of cluster structures characterize not only light α-conjugate nuclei [1–6], but also heavier nuclear systems [7]. Several microscopic models, for instance, the antisymmetrized molecular dynamics [1,2], have very successfully been applied to a description of cluster states in relatively light nuclei. A more general approach based on energy density functionals (EDFs) [8–12] has to be employed in order to study the occurrence and structure of nucleon clusters in medium-heavy and heavy nuclei. Studies based on the latter method have related the conditions for nucleon localization and formation of clusters to the underlying single-nucleon dynamics, geometric shape transitions, and surface effects.

The EDF framework enables a systematic analysis of nucleon localization as a precondition for cluster formation. The Wigner parameter [13] can be used to describe the transition between the nuclear quantum liquid phase and a hybrid phase of cluster states in terms of spatial localization. Such a localization parameter can be microscopically calculated as the ratio of the dispersion of a single-nucleon wave function to the average internucleon distance [9,14]. If the confining nuclear potential is approximated by a three-dimensional harmonic oscillator (HO), the analytic form of the localization parameter exhibits an explicit dependence on the number of nucleons A and the depth of the confining potential V_0. When the spatial dispersion of the single-nucleon wave function is of the same size as the internucleon distance, localization facilitates the formation of clusters [6]. In the present Rapid Communication we aim to explore the dependence of the localization parameter on the specific quantum states occupied by the valence nucleons. A recent study [15] has shown explicitly, using as examples ^{12}C, ^{28}Si, and ^{40}Ca, that single-particle wave functions are localized in light nuclei. Clusters, of course, occur more frequently in light nuclei, but they may also form in heavy systems, such as, for instance, an α-like cluster in ^{212}Po [16]. Can we understand these phenomena in a unified framework?

If the average nuclear potential is approximated by a spherical harmonic oscillator, one obtains the following analytic expression for the localization parameter [9,14,17]:

$$\alpha_{\mathrm{loc}} \simeq \frac{b}{r_0} = \frac{\sqrt{\hbar} A^{1/6}}{\left(2 m V_0 r_0^2\right)^{1/4}}, \tag{1}$$

where $b = \sqrt{\hbar/m\omega_0}$ fm is the oscillator length and $r_0 \simeq 1.25$ fm is the typical internucleon distance determined by nuclear saturation density ($\rho \simeq 0.16$ fm^{-3}). The resulting expression includes the nucleon number A, the mass of the nucleon m, and the depth of the confining potential V_0. As shown in Ref. [14], the oscillator length can be related to the spatial dispersion $\Delta r = \sqrt{\langle r^2 \rangle - \langle r \rangle^2}$: $b \simeq 2\,\Delta r$ for the first s, p, and d HO wave functions. When the dispersion of the single-nucleon wave function is of the same size as the internucleon distance, α_{loc} is on the order of 1, and this facilitates the formation of α clusters. The dependence of the localization parameter on $A^{1/6}$ means that cluster states are preferably formed in lighter nuclei, and the transition from coexisting cluster and mean-field states to a Fermi-liquid state should occur for nuclei with $A \approx 20$–30, in qualitative agreement with experiment.

In finite nuclei the spatial dispersion and, therefore the localization parameter, will explicitly depend on the quantum numbers of specific single-nucleon orbitals. In this Rapid Communication we generalize expression (1) and derive an explicit dependence of the localization parameter on single-nucleon quantum numbers. We also compare the spatial dispersions of the HO wave functions with those obtained in a fully self-consistent microscopic calculation of nuclear ground states and perform a systematic microscopic calculation of

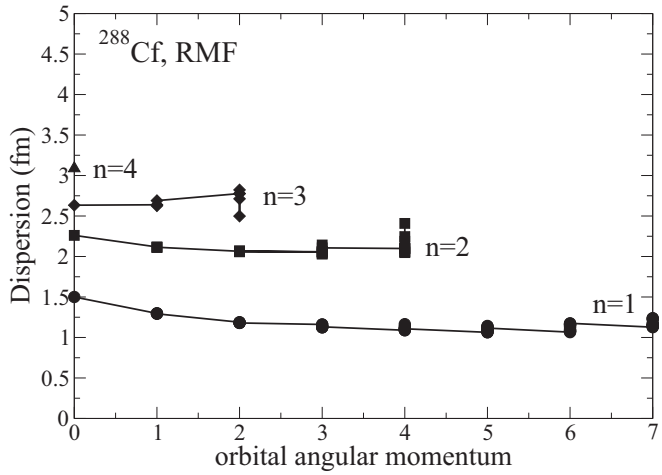

FIG. 1. Radial dispersions Δr of the single-neutron wave functions of ^{288}Cf, obtained in a self-consistent relativistic mean-field (RMF) calculation based on the energy density functional DD-ME2 [18].

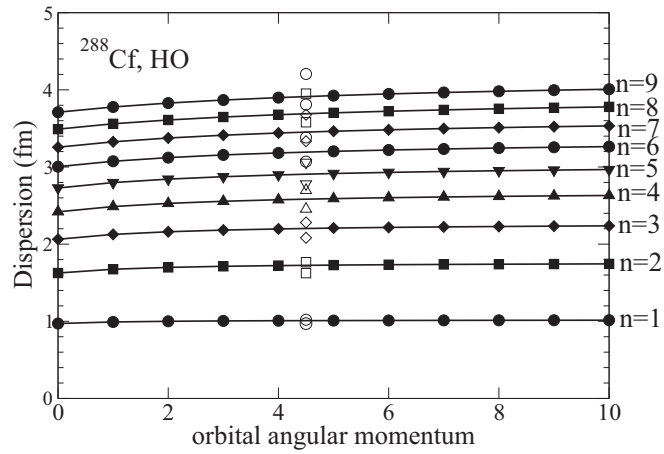

FIG. 2. Radial dispersions Δr of the harmonic-oscillator wave functions of ^{288}Cf, evaluated numerically from Eqs. (2) and (3) (filled symbols) and in the analytical approximation [Eqs. (5) and (8) corresponding to the minimal and maximal values, respectively] (open symbols).

single-nucleon dispersions in axially symmetric nuclei over the entire nuclear chart.

In the first step we perform a systematic microscopic calculation, based on the EDF framework, of dispersions of single-nucleon wave functions in a large nucleus, close to the spherical shape. By considering a heavy spherical nucleus with many occupied levels we can analyze the dependence of the corresponding dispersions on the radial and orbital quantum numbers. Figure 1 displays the spatial dispersions of neutron single-particle states in ^{288}Cf, obtained in a self-consistent RMF calculation using the energy density functional DD-ME2 [18]. The depth of the self-consistent neutron potential is $V_0 = 78.6$ MeV, and the dispersions Δr are plotted as functions of the single-particle radial quantum number n and orbital angular momentum l. One notes a pronounced dependence on the radial quantum number n, whereas the spatial dispersions Δr depend only very weakly on the orbital angular momentum. A particularly interesting result is that for single-neutron states with $n = 1$ the dispersion is of the size of the average internucleon distance. We note that the small splittings between points that correspond to the same orbital angular momenta and radial quantum numbers arise because of deformation: The self-consistent mean-field solution is not fully spherical symmetric (the quadrupole deformation parameter is $\beta_2 = 0.07$).

Next we derive an analytic expression for the dispersion of the single-nucleon wave function for the case when the nuclear potential is approximated by a spherical three-dimensional harmonic oscillator. The HO approach provides a realistic approximation for studies of localization and cluster effects in nuclear systems [19]. The $\langle r^2 \rangle$ term is easy to evaluate and reads

$$\langle r^2 \rangle = b^2\left(N + \tfrac{3}{2}\right) = b^2\left(2n' + l + \tfrac{3}{2}\right), \tag{2}$$

where $N = 2(n-1) + l$ is the principal quantum number and $n' \equiv n - 1$. The $\langle r \rangle$ term is considerably more complicated. Using the HO wave functions, it can be expressed in the following form:

$$\frac{\langle r \rangle}{b} = \sum_{q=0}^{n'} \frac{(-1)^q (l+q+1)!\,\Gamma\left(n'-q-\frac{1}{2}\right)}{q!(n'-q)!\,\Gamma\left(l+q+\frac{3}{2}\right)\Gamma\left(-q-\frac{1}{2}\right)}, \tag{3}$$

where Γ is the Euler function. To compare with the microscopic results shown in Fig. 1, the corresponding dispersions for the single-particle wave functions of the harmonic-oscillator potential of ^{288}Cf are evaluated numerically using Eqs. (2) and (3) and plotted in Fig. 2. The dispersion, of course, increases with the number of radial nodes but shows very little dependence on the orbital angular momentum just as in the case of a fully microscopic calculation. It should be noted that the microscopic dispersion (cf. Fig. 1) is typically 1.2 times larger than the corresponding one in the HO approximation because the actual self-consistent nuclear potential is more diffuse. Indeed, a Woods-Saxon potential can be approximated by a HO with a length of about $1.2b$, thus explaining this ratio.

Therefore, if only $n = 1$ states are occupied in a nucleus, all nucleons have similar and minimal spatial dispersion, on the order of 1 fm. The pronounced localization will favor formation of α-like clusters, whereas the occupation of $n > 1$ states breaks the coherence of spatial localization. Of course, nuclei in which only levels originating from the $n = 1$ spherical states are occupied are the light ones up to about silicon ($Z = 14$, $1s$, $1p$, and $1d$ levels occupied). These are indeed nuclear systems in which cluster structures are empirically most pronounced [20].

To derive a generalization of the expression for the localization parameter in the HO approximation Eq. (1) but now taking explicitly into account the quantum numbers of occupied states, we simplify the n and l dependences in Eq. (3). For $l = 0$ one obtains

$$\frac{\langle r \rangle}{b} = \frac{2}{\sqrt{\pi}} \frac{(2n'+1)!!}{(2n')!!} \simeq \frac{2}{\sqrt{\pi}} \left(\frac{5n'}{4} + 1\right)^{1/2}, \tag{4}$$

where the right-hand side is an accurate approximation with a <1% error for $n' = 20$. Thus, using Eqs. (2) and (4), the $l = 0$ dispersion reads

$$\left(\frac{\Delta r}{b}\right)^2 \simeq \left(2 - \frac{5}{\pi}\right)n' + \left(\frac{3}{2} - \frac{4}{\pi}\right) \simeq 0.4n' + 0.23. \quad (5)$$

Let us now consider the case of large angular momenta l in Eq. (3). In this limit [21],

$$\frac{(l+q+1)!}{\Gamma\left(l+q+\frac{3}{2}\right)} \simeq \sqrt{l} + \frac{1}{\sqrt{l}}\left(\frac{q}{2} + \frac{5}{8}\right), \quad (6)$$

and the expression Eq. (3) reduces to

$$\frac{\langle r\rangle}{b} \simeq \sqrt{l} + \frac{1}{\sqrt{l}}\left(\frac{5}{8} + \frac{3n'}{4}\right). \quad (7)$$

The corresponding dispersion for large l values reads

$$\left(\frac{\Delta r}{b}\right)^2 \simeq \frac{n'}{2} + \frac{1}{4}. \quad (8)$$

The close agreement of the expressions for $l = 0$ [Eq. (5)] and in the large l limit [Eq. (8)] reflects the weak dependence of the HO dispersion on orbital angular momentum. The corresponding dispersions of occupied states of ^{288}Cf: Minimal values corresponding to Eq. (5) and maximal values computed using Eq. (8) are indicated by open symbols in Fig. 2. Both expressions, of course, yield very similar dispersions. Equation (8) implies, as also shown in Fig. 2, that the occupation of an $n = 2$ state leads to a dispersion that is by a factor $\sqrt{3} \sim 1.7$ larger than the one of $n = 1$ states. This corresponds to the case of medium-heavy nuclei, typically above silicon, in which there is no clear evidence of cluster states at low energies and angular momenta.

From Eqs. (1) and (8) we finally derive the approximate expression for the HO localization parameter,

$$\alpha_{\rm loc} = \frac{2\Delta r}{r_0} \simeq \frac{b}{r_0}\sqrt{2n-1} = \frac{\sqrt{\hbar(2n-1)}}{\left(2mV_0r_0^2\right)^{1/4}}A^{1/6}. \quad (9)$$

In nuclei the depth of the confining potential is rather constant as well as the average internucleon distance, hence the two key parameters that determine localization are A and the radial quantum number n. For relatively light nuclei with $A \leqslant 30$ and $n = 1$ states occupied, $\alpha_{\rm loc} \lesssim 1$, and this favors the formation of α-like clusters. In heavier nuclei levels that originate from $n > 1$, spherical states are largely delocalized, and this explains the predominant liquid drop nature of these systems.

An interesting possibility, however, is the formation of individual α-like clusters from valence nucleons in heavy nuclei. We have performed a systematic fully self-consistent relativistic Hartree-Bogoliubov (RHB) [22] calculation of single-nucleon dispersions in axially symmetric nuclei over the entire nuclear chart using the functional DD-ME2. Pairing correlations have been taken into account by employing an interaction that is separable in momentum space and is completely determined by two parameters adjusted to reproduce the empirical bell-shaped pairing gap in symmetric nuclear matter [23]. The Dirac-Hartree-Bogoliubov equations are solved by expanding the nucleon spinors in a large axially symmetric HO basis. The microscopic values of the dispersion Δr have been calculated for each single-particle state. Figure 3 indicates, on the table of nuclides on the N-Z plane, those nuclei in the RHB calculation for which both the neutron and the proton valence states (having an occupation probability larger than 0.1) exhibit a significantly small dispersion on the order of 1 fm. For deformed nuclei it can be shown that these Nilsson levels do originate from $n = 1$ spherical states with the degeneracy raised by deformation. One notices that pronounced localization, as a precondition for the formation of cluster structures, is present in light nuclei but also occurs among valence nucleons in medium-heavy and heavy nuclei, in agreement with empirically known α- and cluster-radioactive nuclei. For instance, a favorable condition for clustering is predicted for ^{212}Po, in accordance with experimental evidence [16]. The EDF-based approach used in this Rapid Communication provides a global interpretation of the occurrence of cluster structures by means of spatial dispersion of single-nucleon wave functions.

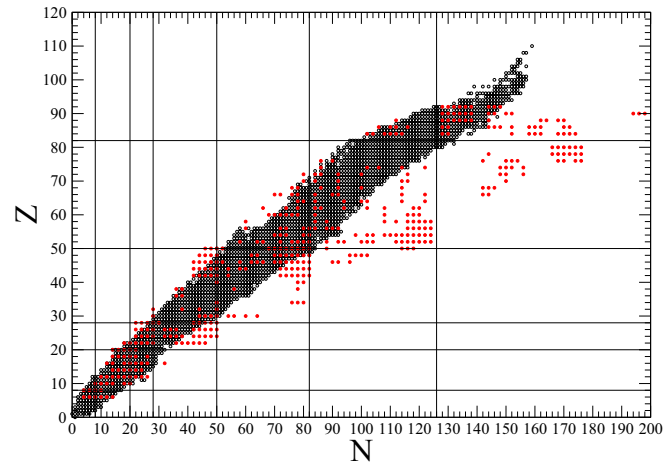

FIG. 3. Microscopic axially symmetric RHB prediction of nuclei that have small radial dispersion of the single-particle states of valence nucleons (red circles), plotted on the background of empirically known nuclides on the N-Z plane. The single-nucleon dispersions have been calculated using the functional DD-ME2 and separable pairing and assuming axial symmetry.

The role of deformation, which is known to favor cluster formation [10,24,25], is illustrated in Fig. 4 where we show the self-consistent mean-field results for ^{20}Ne calculated using the relativistic density functional DD-ME2 in the RMF approach. Pairing does not play an important role for the effect that we consider in this particular nucleus, and it has not been included in the RMF calculation restricted to axial symmetry. Figure 4 displays the occupied single-neutron levels as functions of the axial deformation parameter, the dispersion of the wave function corresponding to the highest level occupied by the two valence neutrons, and the partial intrinsic densities of the valence neutrons for values of deformation that correspond to the peaks and minima of dispersion. In general, the spatial dispersion increases with deformation until a level crossing occurs for the last occupied state. The largest and sharpest increase in the spatial dispersion takes place at the deformation at which a $1/2^+$ state (originating from the $2s_{1/2}$ spherical

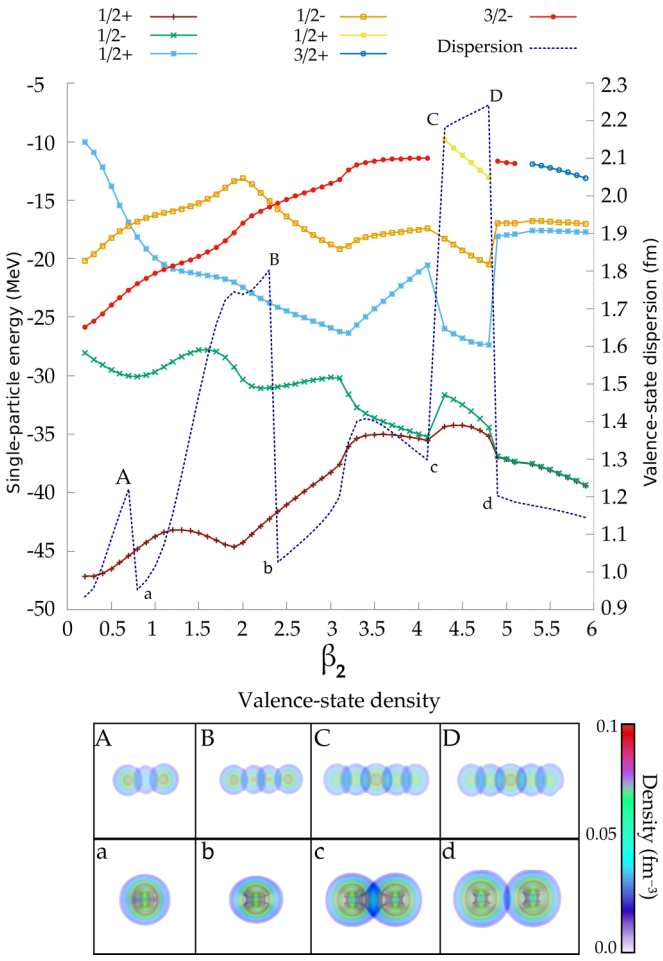

FIG. 4. The occupied single-neutron levels Ω^{π} of ^{20}Ne in the RMF approach as functions of the axial deformation parameter (solid curves), the dispersion of the wave function corresponding to the highest level occupied by the two valence neutrons (blue dotted curve), and the partial intrinsic densities of the valence neutrons for values of deformation that correspond to the peaks and minima of dispersion.

state) becomes occupied. It is remarkable that at this point the dispersion increases by the factor of ~ 1.7, which we encountered above when discussing the filling of the $n = 2$ HO state [cf. Eq. (8) and Fig. 2]. The valence state partial densities exhibit more pronounced localization for small dispersion, whereas the largest spreading is obtained at points C and D at which the $1/2^+$ state becomes the last occupied neutron level.

The present Rapid Communication can also be related to the discussion of (multi)clustering in superdeformed and hyperdeformed states [24,26]. These specific states (ratio of deformed HO frequencies of two and three, respectively) can be described as irreducible representations of SU(3). The magic numbers of super- (hyper-) deformed states are obtained from the sum of two (three) magic numbers of the spherical system. These relations involve small values of radial quantum numbers, and, through Eq. (9), this can be linked to more localized states. The present approach however, as illustrated in Fig. 4, establishes a connection between spatial dispersion and clustering for all deformations rather than only for specific super- and hyperdeformed states.

To summarize, we have used the self-consistent mean-field framework based on nuclear energy density functionals and the spherical harmonic-oscillator approximation for the nuclear potential to analyze the radial dispersion of single-nucleon wave functions. It has been shown that the dispersion exhibits a pronounced dependence on the radial quantum number but essentially does not depend on the orbital angular momentum. In particular, for single-neutron states with $n = 1$ the dispersion is of the size of the average internucleon distance, and the correspondingly small value of the localization parameter $\alpha_{\rm loc}$ indicates a transition between the nuclear quantum liquid phase and a hybrid phase of cluster states that coexists with mean-field states. Based on the HO approximation, we have derived an analytic expression for the localization parameter that, in addition to the dependence on the depth of the nuclear potential and the nucleon number, explicitly takes into account the radial quantum number of occupied single-nucleon states. For $A \leqslant 30$ and $n = 1$ states occupied, $\alpha_{\rm loc} \lesssim 1$, and the formation of α clusters is favored. Although in heavier nuclei levels that originate from $n > 1$ spherical states are largely delocalized, these systems exhibit the quantum liquid phase of nucleonic matter, and individual α-like clusters can be formed from valence nucleons filling Nilsson levels that can be traced back to the $n = 1$ spherical mean-field states. The role of deformation in the evolution of spatial dispersion of single-nucleon levels has been microscopically analyzed in the example of ^{20}Ne, showing the robustness of the present analysis and conclusions. This Rapid Communication provides a general basis for understanding the conditions for cluster formation in light and heavy nuclei.

This Rapid Communication has been supported, in part, by the QuantiXLie Centre of Excellence, a project cofinanced by the Croatian Government and European Union through the European Regional Development Fund—the Competitiveness and Cohesion Operational Programme (Program No. KK.01.1.1.01).

[1] H. Horiuchi, K. Ikeda, and K. Kato, Prog. Theor. Phys. Suppl. **192**, 1 (2012).
[2] M. Kimura, T. Suhara, and Y. Kanada-En'yo, Eur. Phys. J. A **52**, 373 (2016).
[3] N. Itagaki, S. Okabe, K. Ikeda, and I. Tanihata, Phys. Rev. C **64**, 014301 (2001).
[4] P.-G. Reinhard, J. A. Maruhn, A. S. Umar, and V. E. Oberacker, Phys. Rev. C **83**, 034312 (2011).
[5] A. Tohsaki, H. Horiuchi, P. Schuck, and G. Röpke, Rev. Mod. Phys. **89**, 011002 (2017).
[6] J. P. Ebran, E. Khan, T. Nikšić, and D. Vretenar, J. Phys. G **44**, 103001 (2017).

[7] C. Beck, *Clusters in Nuclei*, Lecture Notes in Physics Vols. 818, 848, and 875 (Springer, Berlin, 2010–2014).
[8] P. Arumugam, B. K. Sharma, S. K. Patra, and R. K. Gupta, Phys. Rev. C **71**, 064308 (2005).
[9] J. P. Ebran, E. Khan, T. Nikšić, and D. Vretenar, Nature (London) **487**, 341 (2012).
[10] J. P. Ebran, E. Khan, T. Nikšić, and D. Vretenar, Phys. Rev. C **90**, 054329 (2014).
[11] P. Marevic, J. P. Ebran, E. Khan, T. Nikšić, and D. Vretenar, Phys. Rev. C **97**, 024334 (2018).
[12] P. Jerabek, B. Schuetrumpf, P. Schwerdtfeger, and W. Nazarewicz, Phys. Rev. Lett. **120**, 053001 (2018).
[13] E. P. Wigner, Phys. Rev. **46**, 1002 (1934).
[14] J. P. Ebran, E. Khan, T. Nikšić, and D. Vretenar, Phys. Rev. C **87**, 044307 (2013).
[15] A. V. Afanasjev and H. Abusara, Phys. Rev. C **97**, 024329 (2018).
[16] A. Astier, P. Petkov, M.-G. Porquet, D. S. Delion, and P. Schuck, Phys. Rev. Lett. **104**, 042701 (2010).
[17] J. P. Ebran, E. Khan, T. Nikšić, and D. Vretenar, Phys. Rev. C **89**, 031303(R) (2014).
[18] G. A. Lalazissis, T. Nikšić, D. Vretenar, and P. Ring, Phys. Rev. C **71**, 024312 (2005).
[19] B. Schuetrumpf, C. Zhang, and W. Nazarewicz, *Nuclear Particle Correlations and Cluster Physics* (World Scientific, singapore, 2017), p. 135.
[20] W. v. Oertzen, M. Freer, and Y. Kanada-En'Yo, Phys. Rep. **432**, 43 (2006).
[21] M. Abramovitz, in *Handbook of Mathematical Functions*, edited by M. Abramovitz and I. Stegun (Dover, Mineola, NY, 1964).
[22] D. Vretenar, A. V. Afanasjev, G. A. Lalazissis, and P. Ring, Phys. Rep. **409**, 101 (2005).
[23] T. Nikšić, P. Ring, D. Vretenar, Y. Tian, and Z. Y. Ma, Phys. Rev. C **81**, 054318 (2010).
[24] W. D. M. Rae, Int. J. Mod. Phys. **3**, 1343 (1988).
[25] C. L. Zhang, B. Schuetrumpf, and W. Nazarewicz, Phys. Rev. C **94**, 064323 (2016).
[26] W. Nazarewicz and J. Dobaczewski, Phys. Rev. Lett. **68**, 154 (1992).